# Infinitesimal incommensurate stripe phase in an axial next-nearest-neighbor Ising model in two dimensions

Takashi Shirahata and Tota Nakamura
*Department of Applied Physics, Tohoku University, Sendai, Miyagi 980-8579, Japan*
(Received 20 February 2001; revised manuscript received 2 August 2001; published 6 December 2001)

An axial next-nearest-neighbor Ising model is studied by using the nonequilibrium relaxation method. We find that the incommensurate stripe phase between the ordered phase and the paramagnetic phase is negligibly narrow or may vanish in the thermodynamic limit. The phase transition is the second-order transition if approached from the ordered phase, and it is of the Kosterlitz-Thouless type if approached from the paramagnetic phase. Both transition temperatures coincide with each other within the numerical errors. The incommensurate phase which has been observed previously is a paramagnetic phase with a very long correlation length (typically $\xi \geqslant 500$). We could resolve this phase by treating very large systems ($\sim 6400 \times 6400$), which is first made possible by employing the present method.

DOI: 10.1103/PhysRevB.65.024402 PACS number(s): 75.10.Hk, 64.70.Rh, 75.40.Mg

## I. INTRODUCTION

Of late, incommensurate (IC) stripe structures have been interesting subjects in various physical phenomena. As the typical examples, we may list an alloy $Er_{90}Y_{10-x}La_x$ which contains heavy rare earth metals Er, Tm,[1,2] the incommensurate phase of dielectric material such as $Pb(Zr_{1-x}Ti_x)O_3$ and $NaNO_2$,[3–7] and the stripe structure in $CuO_2$ planes of oxide superconductors.[8] In $Er_{90}Y_{10-x}La_x$, the longitudinal incommensurate oscillatory phase appears between the paramagnetic phase and the ordered phase. The aligned holes (domain walls) separate antiferromagnetic stripes in $CuO_2$ planes of oxide superconductors, then the spin and charge are modulated. In such systems, cooperative effects of fluctuation and frustration are considered to play important roles. Thus, we sometimes treat them with the axial next-nearest-neighbor Ising (ANNNI) model as the simplified theoretical model. For instance, when a uniaxial anisotropy is strong in the dielectric material, the Hamiltonian is equivalent to the ANNNI model if we only consider the dipole interactions up to the next-nearest-neighbor distance. The phase diagram of $Pb(Zr_{1-x}Ti_x)O_3$ obtained by experiments[3] agrees with that of the three-dimensional ANNNI model obtained by the mean-field approximation.[9] In copper oxide materials $Ca_8La_6Cu_{24}O_{41}$ and $Ca_2Y_2Cu_5O_{10}$, the Cu-O-Cu chains with ferromagnetic nearest-neighbor and antiferromagnetic next-nearest-neighbor interactions are aligned on two-dimensional planes whose interchain interactions are antiferromagnetic. Furthermore, the spins on this plane are predicted to have a strong Ising anisotropy.[10,11] Consequently, we may treat these copper oxide planes as the two-dimensional ANNNI model, between which the conduction electron planes exist.

In the ANNNI model, there are exchange interactions up to the next-nearest-neighbor pairs along one axis, while there are only the nearest-neighbor interactions along the other axes. Most commonly, we take a convention that the nearest-neighbor interactions are ferromagnetic and the next-nearest-neighbor ones are antiferromagnetic, which cause frustration. When the next-nearest-neighbor interactions (frustration) are weak, a ferromagnetic state is the ground state, and a paramagnetic-ferromagnetic phase transition occurs. On the other hand, when frustration is strong, the ground state is the *antiphase* state (abbreviated by $\langle 2 \rangle$), which is a commensurate (C) stripe structure of two up spins and two down spins such as $\uparrow\uparrow\downarrow\downarrow\uparrow\uparrow$. It is widely accepted that the incommensurate stripe phase exists between the paramagnetic phase and the antiphase, and that the successive phase transitions (paramagnetic-IC-antiphase) take place; there is a ''finite'' incommensurate phase where the up spins and down spins are aligned with a period longer than two.

Although only a topology of the phase diagram is known by the mean-field approximation in the three-dimensional model,[9] estimates for the phase transition temperatures in two dimensions have been done by several approximation theories[12–17] and numerical simulations.[18–20] However, values of the phase transition temperatures scatter much depending on the methods employed. One of the reasons that make the estimate difficult is a lack of a reliable numerical simulation. Because of frustration, the correlation time of Monte Carlo (MC) simulations becomes very long near the critical point in large systems. Thus, we are hardly able to reach thermal equilibrium states within reasonable time steps. A powerful method called a cluster heat bath (CHB) method[20] was developed to reduce the correlation time, however, the system size accessible by this method is restricted up to about $64 \times 128$ lattice sites.

Recently, a new method using a MC simulation has been developed: the nonequilibrium relaxation (NER) method.[21,22] We are able to understand phase transitions from the differences of behaviors in nonequilibrium relaxation processes, which have been discarded in conventional MC simulations. Since we do not wait until the equilibrium is realized, we can use the CPU time to enlarge the system sizes. Therefore, it makes possible to treat large systems that cannot be possible by other methods. Accordingly, there is expected to be little finite-size effect in the obtained data, and thus we can regard them as those of the infinite systems. For the reasons stated above, the NER method can be effective especially in systems with a slow dynamics which a very long equilibration is necessary.[23–31]

 ©2001 The American Physical Society

In this paper, we study the two-dimensional ANNNI model by the NER method in order to determine the successive phase transition temperatures. However, the obtained results suggest that the IC phase may disappear within limits of numerical errors. Moreover, we found a very exotic phase transition, which seems to be the Kosterlitz-Thouless (KT) transition[32] if it is observed from the high-temperature side, and seems to be the second-order transition if observed from the low-temperature side. This evidence suggests that the frustration parameter does not serve as an asymmetric parameter[33–35] which explicitly favors the IC structure.

We describe the model Hamiltonian and the NER method in Sec. II, and present simulational results in Sec. III. Section IV is devoted to conclusions.

## II. MODEL AND METHOD

### A. Two-dimensional ANNNI model

The two-dimensional ANNNI model is described by the following Hamiltonian:

$$\mathcal{H}=-\sum_{x,y}\left(J_0 S_{x,y}S_{x+1,y}+J_1 S_{x,y}S_{x,y+1}+J_2 S_{x,y}S_{x,y+2}\right), \tag{1}$$

where $J_0(>0)$ is the nearest-neighbor interaction along the chain direction, which is the direction that has no frustration. $J_1(>0)$ and $J_2(<0)$ are respectively the nearest-neighbor and the next-nearest-neighbor interactions along a direction perpendicular to the chain direction (axial direction that has frustration), and $S_{x,y}=\pm 1$. In this paper, we fix $J_0=J_1$ for simplicity, and impose the open boundary conditions along the axial ($y$) direction, while we use the periodic boundary conditions along the chain ($x$) direction. We define a ratio between the nearest and the next-nearest-neighbor interactions along the axial direction as $\kappa(=-J_2/J_1)$. Our interest is restricted to the region $\kappa>1/2$, where the successive phase transitions (antiphase→IC→paramagnetic) has been considered to occur.

The fermion approximations assumed that the system has straight domain walls along the chain direction at the intermediate temperatures.[13] That is, domains whose periods are longer than two appear among the commensurate antiphase domains. In this case, the spin structure becomes incommensurate along the axial direction, while the spins along the chain direction order ferromagnetically. On the other hand, it was postulated that domain walls run along the axial direction in the interface free energy method of Müller-Hartmann and Zittartz (MHZ).[12,14] Namely, the correlation of spins ordered ferromagnetically along the chain direction is destroyed by these domain walls.

Sato and Matsubara[20] discussed using the CHB simulation that the transition temperature ($T_{c2}$) between the antiphase and the IC phase agrees with that of the free-fermion approximation while the transition temperature ($T_{c1}$) between the IC phase and the paramagnetic phase is close to $T_{c2}$ obtained by MHZ. Thus, they considered that the domain walls penetrate into the system along the chain direction at $T_{c2}$ as the temperature increases from the ground state. The ferromagnetic correlations along the chain direction remain until they are destroyed at $T_{c1}$ and the paramagnetic state is realized. This idea means that the IC phase exists between the penetration of incommensurate domains in the axial direction and the disappearance of the ferromagnetic chain correlation. Therefore, the spin structure along the axial direction is incommensurate, while it is ferromagnetic along the chain direction in the IC phase. It has been considered that the phase transition between the paramagnetic phase and the IC phase is the KT transition and that between the IC phase and the antiphase is the second-order transition.

We consider following two quantities to clarify the phase transitions. One is the antiphase magnetization defined by

$$m_{\langle 2\rangle}(t)=\frac{1}{N}\sum_{x,y} S_{x,y}(\langle 2\rangle)S_{x,y}(t), \tag{2}$$

where $N$ is the total number of spins in the system, $S_{x,y}(t)$ denotes the spin value of the site $(x,y)$ at time $t$, and $S_{x,y}(\langle 2\rangle)$ represents the antiphase ordered state. The antiphase magnetization takes a finite value in the antiphase, but vanishes in the IC phase and the paramagnetic phase, since the domain walls destroy the antiphase state at the lower transition temperature, $T_{c2}$. Therefore, this parameter is employed to estimate $T_{c2}$.

Here, we should note that the antiphase magnetization is not a relevant order parameter that decays algebraically at the transition temperature. Since the elementary excitation is a domain wall which readily percolates the chain direction, the antiphase magnetization decays exponentially once the domain wall penetrate into the system. Usually, the density of the domain walls has been used as an order parameter. This parameter is considered to diverge algebraically at the transition temperature as $(T-T_{c2})^{\beta}$, which is equivalent to that the correlation length diverges algebraically as $\xi\sim(T-T_{c2})^{-\nu}$. In this point, the phase transition between the IC phase and the antiphase is the second-order transition. In the Monte Carlo simulations, the correlation length is related to the characteristic time as $\tau\sim\xi^z$, where $z$ is called the dynamic exponent. Therefore, the characteristic time also diverges at $T_{c2}$ as $\tau\sim(T-T_{c2})^{-z\nu}$. We can extract it from the relaxation of the antiphase magnetization: the time that the antiphase magnetization begins to decay exponentially is the characteristic time that the domain wall penetrates into the system. We execute the finite-time scaling to obtain the characteristic time at each temperature and estimate $T_{c2}$ as its diverging temperature. A concrete procedure of the finite-time scaling is explained in Sec. II D. The antiphase magnetization is an extensive variable so that it shows better accuracy as the system size is enlarged because of the self averaging. Thus, we use the antiphase magnetization to estimate the lower transition temperature $T_{c2}$.

The other quantity is the layer magnetization defined as

$$m_l(t)=\frac{1}{L_y}\sum_{y=1}^{L_y}\left(\frac{1}{L_x}\sum_{x=1}^{L_x} S_{x,y}(t)\right)^2, \tag{3}$$

where $L_x$ and $L_y$ are the length of the system along the chain and the axial direction, respectively. The layer magnetization

reflects the spin order along the chain direction. In the IC phase, the incommensuration is realized in the axial direction. The spin arrangement along the chain direction should order ferromagnetically or at least be critical. The free energy of this state, which is of the order of $-L^{1+1/\nu}$, is always lower than that of the state with the spins disordered only along the chain direction, which is of the order of $-L$, if $\nu$ is positive. Accordingly, the layer magnetization vanishes exponentially in the paramagnetic phase, but takes a finite value or behaves in a power law in the IC phase. Therefore, this order parameter is used to estimate the upper transition temperature $T_{c1}$. We determine the transition temperatures by using these two quantities in this paper.

### B. Nonequilibrium relaxation (NER) method (Refs. 21,22,30,31)

Phase transitions occur in the infinite-size limit ($L\to\infty$) and in the equilibrium limit ($t\to\infty$). Because we cannot take both limits at the same time in the simulation, the equilibrium limit has been taken first conventionally, and then, we take the infinite-size limit by using the finite-size scaling. However, the dynamics of the simulations are very slow in the frustrated systems, which causes a very large correlation time. From a time-space relation $\tau\sim\xi^z$, this means that the correlation length is also very large. As will be mentioned in Sec. III, we estimate the correlation length $\xi_x\sim 500$, for $\kappa=0.8$ and $T=1.40$, which resides in the IC phase of previous phase diagram. In this situation, reliability of the finite-size scaling might become doubtful. In this paper, we follow a completely alternative approach to the thermodynamic limit, i.e., we observe the relaxation of the infinite-size system to the equilibrium state. In order to extract the equilibrium properties, the finite-time scaling analysis is utilized instead of the conventional finite-size scaling. This approach is known as the nonequilibrium relaxation (NER) method.[21,22,30,31] Actually, we prepare a very large lattice and observe the relaxation of physical quantities. The simulations are stopped before the finite-size effect appears. Accordingly we can regard the systems as the infinite systems.

Using the NER method, we can estimate the phase transition temperature and the critical exponents by examining behaviors of the relaxation processes to the thermal equilibrium state (nonequilibrium relaxation processes). The analysis is based on the dynamic finite-size scaling hypothesis of the free energy that

$$F(\varepsilon,h,L,t)=L^{-d}\tilde{F}(\varepsilon L^{1/\nu},hL^{d-\beta/\nu},tL^{-z}), \tag{4}$$

where $\varepsilon[\equiv(T-T_c)/T_c],h,L,t$ are the relative temperature, the symmetry breaking field, the system size, and time, respectively. $\nu$ and $\beta$ denote static exponents, while $z$ is a dynamic exponent, and $d$ is a dimension of space.[36] The order parameter is given by a derivative of the free energy with the field

$$\begin{aligned} m(t)&\sim \left.\frac{\partial F}{\partial h}\right|_{h=0} \\ &=L^{-\beta/\nu}\bar{F}(\varepsilon L^{1/\nu},tL^{-z}) \\ &=t^{-\beta/z\nu}\hat{F}(\varepsilon t^{1/z\nu}) \\ &\propto t^{-\beta/z\nu}(\varepsilon=0,L\to\infty), \end{aligned} \tag{5}$$

where we have set $L\sim t^{1/z}$ at the transition point ($\varepsilon=0$) because the characteristic time scale $\tau$ and the correlation length $\xi$ should scale as $\xi\sim\tau^{1/z}$. Equation (5) describes that the order parameter decays in a power law with time at the transition temperature. On the other hand, the order parameter behaves exponentially at temperatures away from the critical point. Thus, we are able to estimate $T_c$ by this difference. Actually, we measure the order parameter $m(t)$ at each MC step ($t$) started from an ordered spin configuration at a given temperature. We repeat this MC run by changing the random number seeds, and $m(t)$ is averaged over these independent MC runs. The temperature at which the $m(t)$ curve decays in a power law is the transition temperature.

We use the local exponent to ascertain whether the order parameter decays in a power law or exponentially, which is defined by

$$\lambda(t)=\left|\frac{d\ln m(t)}{d\ln t}\right|. \tag{6}$$

When we plot the local exponent against $1/t$, it diverges to infinity for $T>T_c$, it converges to zero for $T<T_c$ and to a finite value ($\neq 0$) at $T=T_c$ in the limit of $1/t\to 0$. The upper bound of $T_c$ is the lowest temperature that $\lambda(t)$ diverges, and the lower bound is the highest temperature that $\lambda(t)$ decays to zero. The convergent value of the local exponent at $T=T_c$ is the critical exponent $\lambda=\beta/z\nu$ from Eq. (5).

### C. NER of fluctuation (Refs. 22,23,37,38)

Here, we describe the NER of fluctuation. The susceptibility is written by differentiating Eq. (4) with the symmetry breaking field twice,

$$\left.\frac{\partial^2 F}{\partial h^2}\right|_{h=0}\propto\langle m(t)^2\rangle-\langle m(t)\rangle^2\propto t^{d/z-2\beta/z\nu}=t^{\gamma/z\nu}, \tag{7}$$

where we have used the scaling relations

$$\begin{cases} d\nu=2-\alpha, \\ \alpha+2\beta+\gamma=2. \end{cases} \tag{8}$$

The susceptibility diverges in a power law at the transition temperature. Thus, we are able to estimate the transition temperature and the critical exponents from the susceptibility. It is also noticed that the NER of fluctuation does not require us to start with a symmetry-broken ordered state. The quantity of fluctuation always takes a definite value and diverges at $T_c$ even though the symmetry is not spontaneously broken. Therefore, we can start from a paramagnetic state or any state in this scheme. This is especially useful when an or-

dered state is not known yet, or it is difficult to realize. The layer magnetization defined by Eq. (3) is equivalent to the second derivative with respect to a local field along a single chain in the paramagnetic phase. When the simulation starts from the antiphase, the first derivative term remains finite in the NER process even though the temperature is in the paramagnetic phase. Therefore, the layer magnetization is not regarded as the susceptibility. The NER of the layer magnetization is within a scheme of the NER of fluctuation, only when the simulation is started from the paramagnetic state.

### D. Finite-time scaling (Refs. 30,31)

In case when the NER function does not begin to decay algebraically within a reasonable time, it is difficult or almost impossible to estimate the transition temperature directly by the local exponent. Even in such a situation, we are able to determine it by using the finite-time scaling analysis, which is a direct interpretation of the finite-size scaling by a relation $\xi \sim \tau^{1/z}$. We present the finite-time scaling relation as follows:

$$m(\varepsilon,t) = t^{-\lambda}\hat{m}[t/\tau(\varepsilon)], \tag{9}$$

where $\lambda = \beta/z\nu$, and $\tau(\varepsilon)$ denotes a relaxation time at the relative temperature $\varepsilon$. Since the relaxation time diverges algebraically in the case of the second-order phase transitions, the relation between the relaxation time and the relative temperature is described by

$$\tau(\varepsilon) = A\varepsilon^{-z\nu}. \tag{10}$$

On the other hand, in the case of the KT transition,[32] it is considered that the relaxation time diverges exponentially, which we assume that

$$\tau(\varepsilon) = A\exp(B/\sqrt{\varepsilon}). \tag{11}$$

Now, we describe how we actually estimate the transition temperature by using Eqs. (9)–(11). We use only data which is clearly in the paramagnetic phase $T > T_c$. First, we plot $m(t)t^{\lambda}$ at various temperature against $t/\tau(\varepsilon)$ by using Eq. (9) to determine $\lambda$ and $\tau(\varepsilon)$ so that all data points fall on a single curve. Next, we plot $\tau(\varepsilon)$ against $\varepsilon$, and fit the points to a smooth curve as we change $T_c$ and $z\nu$ by using Eq. (10) for the second-order transition. In the KT-transition case, we use Eq. (11) instead. The temperature at which the least-square fitting error becomes minimum is the most probable estimate for $T_c$. The phase transition between the paramagnetic phase and the IC phase is the KT transition and that between the IC phase and the antiphase is the second-order transition in the two-dimensional ANNNI model. Therefore, we use Eq. (11) for the upper transition temperature, and Eq. (10) for the lower one.

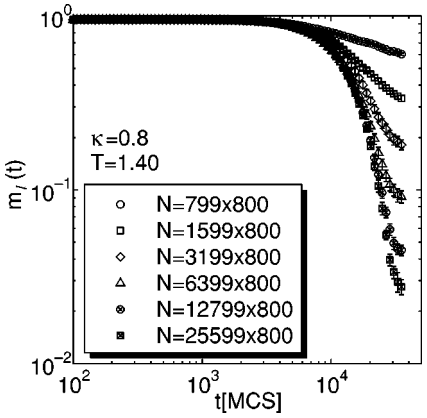


FIG. 1. The finite-size effect of the layer magnetization for $\kappa = 0.8$ at $T = 1.4$. Length along an axial direction is fixed to 800, while that along a chain direction is varied from 799 to 25 599. The converging value is roughly considered as $\xi_x/L_x$, from which we derived the correlation length along the ferromagnetic chain direction as $\xi_x \sim 500$.

## III. SIMULATION AND RESULTS

### A. NER from the antiphase state

We examine the phase transition temperature for $\kappa = 0.6$ and 0.8. The temperature is measured in a unit of $J_1$. Here, the NER of two quantities are presented by the simulation started from the antiphase state.

TABLE I. Comparison of the present estimate of $T_{c1}$ and $T_{c2}$ for $\kappa = 0.6$ and $\kappa = 0.8$ with the previous ones.

| | $\kappa = 0.6$ | | $\kappa = 0.8$ | |
|---|---|---|---|---|
| Present results/References | $T_{c1}$ | $T_{c2}$ | $T_{c1}$ | $T_{c2}$ |
| NER from $T=0$ (scaling) | 0.89(2) | 0.89(2) | 1.31(2) | 1.32(2) |
| NER from $T=\infty$ (local exponent) | 0.90(2) | | 1.325(25) | |
| NER from $T=\infty$ (scaling) | 0.890(15) | | 1.300(13) | |
| Ref. 13 | ~1.20 | ~0.91 | ~1.45 | ~1.30 |
| Ref. 19 | ~1.40 | ~1.00 | ~1.70 | ~1.50 |
| Ref. 14 | | ~1.10 | | ~1.50 |
| Ref. 15 | ~1.35 | ~1.05 | ~1.60 | |
| Ref. 16 | ~1.40 | ~1.05 | ~1.65 | ~1.35 |
| Ref. 17 | ~1.64 | 0.91(1) | ~1.95 | |
| Ref. 20 | 1.16(4) | ~0.91 | ~1.60 | ~1.35 |

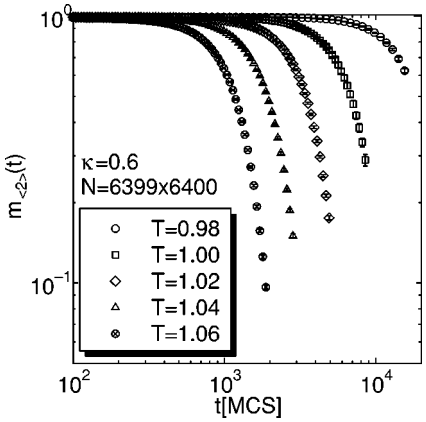


FIG. 2. The NER of the antiphase magnetization $m_{\langle 2\rangle}(t)$ for $\kappa=0.6$. The system size is $N=6399\times6400$. The antiphase magnetization clearly decays exponentially at $T\geqslant0.98$.

First, we observe the NER of the layer magnetization to check the relation between the finite size $L_x$ and the correlation length $\xi_x$ along the chain direction. We change the size along the chain direction from $L_x=799$ to $L_x=25599$, while the length along the axial direction is fixed to $L_y=800$. Figure 1 shows the NER of the layer magnetization, Eq. (3), for $\kappa=0.8$ and $T=1.40$. This temperature belongs to the IC phase (KT phase) in previous investigations as summarized in Table I. When the system size is small ($N=799\times800$), the relaxation roughly looks like a power-law decay, which misled us to the KT phase. As the system becomes larger, the relaxation exhibits an exponential decay confirming us that the system is in the paramagnetic phase. Note that the convergence to a finite value is due to the finite-size effect. By its definition, the equilibrium value of the layer magnetization is roughly estimated as $\xi_x/L_x$ in the paramagnetic phase. As shown in Fig. 1, the convergence value takes a half value if the system size is doubled. Thus, we can estimate the correlation length $\xi_x\sim500$ in this system. From this figure, we can also understand the relation between the finite size effect and the time effect; the effective time that the system behaves as the infinite size. For example, it is about 15 000 MCS in the system with $L_x=6399$. After this time scale, finite size effect appears in dynamics. In this subsection, we use the lattice of $N=6399\times6400$ and determine the observing time at each temperature until which the relaxation curve do not begin to bend to an equilibrium value. We average $24\sim32$ independent MC runs at each temperature.

Figure 2 is a raw data of the NER of the antiphase magnetization, Eq. (2), for $\kappa=0.6$. At all the temperatures, the antiphase magnetization clearly decays exponentially, which guarantees that the transition temperature must be lower than 0.98. As mentioned in Sec. II A, the antiphase magnetization is not a relevant order parameter, and so it decays exponentially as soon as domain walls penetrate into the system. Therefore, we estimate the transition temperature by using the finite-time scaling. At first, we determine the exponent, $\lambda$, and the relaxation time, $\tau_{\langle 2\rangle}(\varepsilon)$, at each temperature so that the scaled data, $m_{\langle 2\rangle}(t)t^{\lambda}$, fall on a single scaling function when plotted against $t/\tau_{\langle 2\rangle}(\varepsilon)$ [Fig. 3(a)]. Here, the relaxation times are normalized by the value of $T=1.06$, and

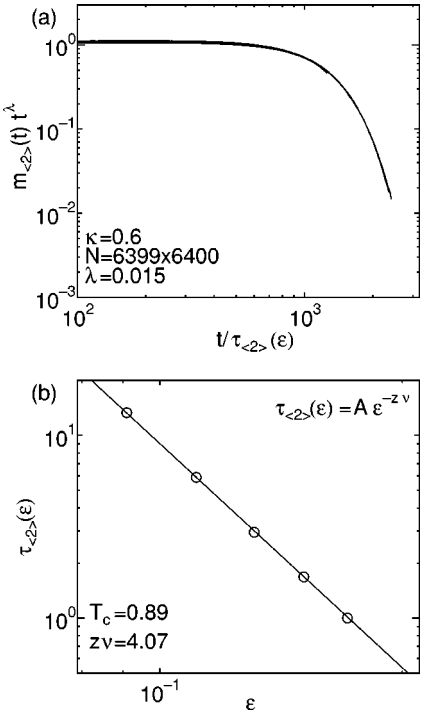


FIG. 3. (a) The finite-time scaling of the antiphase magnetization for $\kappa=0.6$, where $\lambda=0.015$. We use the data at five temperatures ranging $T=0.98$–$1.06$. (b) The least-square fitting of the relaxation time $\tau_{\langle 2\rangle}(\varepsilon)$, by Eq. (10), where we obtain $T_{c2}=0.89\pm0.02$, $z\nu=4.07$.

are listed in Table II. The exponent $\lambda$ that gives best scaling is $\lambda=0.015$. Excellence of the scaling shown in Fig. 3 may yield the validity of the finite-time scaling hypothesis.

Next, we estimate $T_{c2}$ by Eq. (10) because it is predicted that the phase transition between the antiphase and the IC phase is the second-order. We plot $\tau_{\langle 2\rangle}(\varepsilon)$ against $\varepsilon[=(T-T_{c2})/T_{c2}]$ as changing $T_{c2}$ and find a $T_{c2}$ that gives the best linearity in the log-log scale as shown in Fig. 3(b). We obtain $T_{c2}=0.89\pm0.02$ and $z\nu=4.07$. The error $\pm0.02$ is a range of temperature in which the data points clearly fall on the fitting line. The exponent has a range within which we can perform a good scaling as $\lambda=0.000$–$0.030$. The transition temperature takes the same value irrespective of the choice of $\lambda$. Evidence such as the algebraic divergence of $\tau_{\langle 2\rangle}(\varepsilon)$ and excellence of the finite-time scaling support that this transition is the second order. This is a clear distinction from the three dimensional model, where the lower transition is considered as the first order.

We estimate the upper transition temperature $T_{c1}$ using the layer magnetization, Eq. (3), in the same way as mentioned above. Figure 4 shows raw data of the NER of the layer magnetization $m_l(t)$, for $\kappa=0.6$. Here, the layer magnetization clearly decays exponentially, and thus the $T_{c2}$ must be less than 0.98. The finite-time scaling is shown in Fig. 5(a). The obtained relaxation time $\tau_l(\varepsilon)$ is also presented in Table II. Since it is predicted that the phase transition between the IC phase and the paramagnetic phase is the KT transition, we fitted $\tau_l(\varepsilon)$ by Eq. (11) in Fig. 5(b), by which we obtain $T_{c1}=0.89\pm0.02$ and $B=3.44$. If we as-

TABLE II. The relation between the temperatures $T$ and the relaxation time $\tau_{\langle 2\rangle}(\varepsilon)$ of the antiphase magnetization $m_{\langle 2\rangle}(t)$ and the relaxation time $\tau_l(\varepsilon)$ of the layer magnetization $m_l(t)$ for $\kappa=0.6$ and 0.8. The relaxation time is scaled so that a value at the highest temperature becomes unity.

| | $\kappa=0.6$ | | | | $\kappa=0.8$ | | |
|---|---|---|---|---|---|---|---|
| $T$ | $\tau_{\langle 2\rangle}(\varepsilon)$ (from $T=0$) | $\tau_l(\varepsilon)$ (from $T=0$) | $\tau_l(\varepsilon)$ (from $T=\infty$) | $T$ | $\tau_{\langle 2\rangle}(\varepsilon)$ (from $T=0$) | $\tau_l(\varepsilon)$ (from $T=0$) | $\tau_l(\varepsilon)$ (from $T=\infty$) |
| 1.06 | 1.000 | 1.000 | | 1.50 | | | 1.000 |
| 1.04 | 1.680 | 1.656 | | 1.48 | 1.000 | 1.000 | |
| 1.02 | 2.950 | 3.025 | | 1.46 | 1.713 | 1.715 | |
| 1.00 | 5.889 | 6.145 | 1.000 | 1.44 | 3.033 | 3.140 | |
| 0.98 | 13.301 | 16.657 | | 1.42 | 6.264 | 6.889 | |
| 0.97 | | | 3.202 | 1.40 | 14.822 | 20.190 | 17.503 |
| 0.95 | | | 11.103 | 1.35 | | | 752.314 |
| 0.92 | | | 500.115 | | | | |

sumed that the phase transition is the second-order transition, and performed the fitting by Eq. (10), the estimated $T_{c1}$ becomes far from a physically meaningful value. In consequence, we confirm that the upper phase transition is of the KT type. Actually, Sato and Matsubara[20] performed the finite-size scaling of the layer magnetization supposing

$$m_l \times L^{\eta} = Y[L^{-1}\exp(B\varepsilon^{-0.5})], \tag{12}$$

which gave $T_{c1}=1.16$ and $\eta=0.25$ for $\kappa=0.6$. This scaling form is equivalent to the finite-time scaling, Eqs. (9) and (11), if we admit $L=t^{1/z}$ and $\lambda=\eta/z$. The difference of the obtained transition temperatures can be attributed to the difference of the system sizes. We estimate $\lambda=0.015$ by minimizing the normalized residual, however, this value does not correspond to $(2-\eta)/z$. Because we start simulations from the antiphase state, the layer magnetization contains contributions from the antiphase magnetization, $\langle m_{\langle 2\rangle}\rangle^2$.

We have obtained the $T_{c2}$ and the $T_{c1}$ for $\kappa=0.8$ in the same way. In the finite-time scaling plot, we used the data at five temperature ranging $T=1.40\sim1.48$, and obtained $T_{c2}=1.32\pm0.02$ and $T_{c1}=1.31\pm0.02$.

The phase transition temperatures, $T_{c1}$ and $T_{c2}$, coincide within limits of error both for $\kappa=0.6$ and 0.8. This means the IC phase may vanish in the thermodynamic limit. Because this is a rather daring conclusion, we must confirm it from another point of view. Actually, it might be dangerous to estimate the transition temperature between the paramagnetic phase and the IC phase started from the ground state.

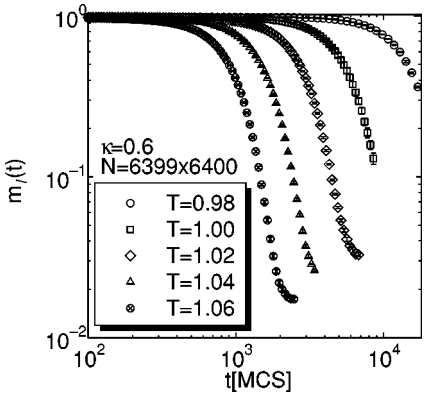


FIG. 4. The NER of the layer magnetization $m_l(t)$, for $\kappa=0.6$. The size of system is $N=6399\times6400$. The layer magnetization clearly decays exponentially at $T\geqslant0.98$.

### B. NER from the paramagnetic state

We start the simulation from the paramagnetic state and observe the NER of fluctuation; the layer magnetization. Since the observable is a quantity of fluctuation, it is necessary to take much more sample averages compared to the

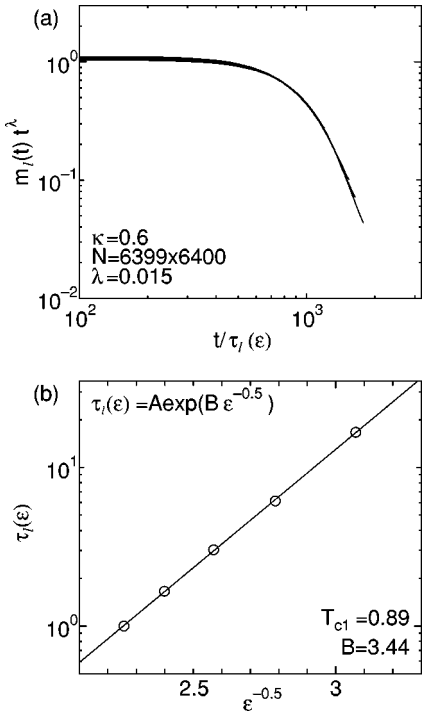


FIG. 5. (a) The finite-time scaling of the layer magnetization for $\kappa=0.6$, where $\lambda=0.015$. The data of five temperatures ranging $T=0.98-1.06$ are plotted together. (b) The least-square fitting of the relaxation time $\tau_l(\varepsilon)$, by Eq. (11), where we obtain $T_{c1}=0.89\pm0.02$, $B=3.44$.

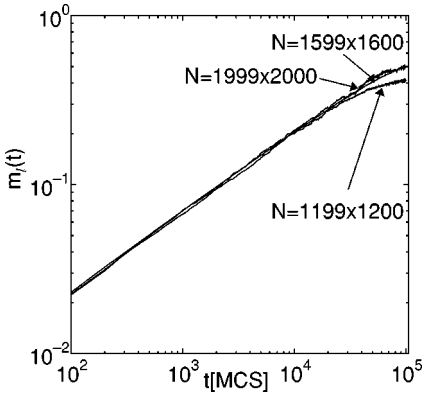


FIG. 6. Size dependence of the NER of layer magnetization $m_l(t)$ at $T=0.92$ and $\kappa=0.6$. Three curves of $N=1999\times2000$, $N=1599\times1600$, and $N=1199\times1200$ fall on the same line until 25 000 MCS. Then, the curve of $N=1199\times1200$ deviates down from the other two curves, which remain consistent until 100 000 MCS. We discard the data of $N=1199\times1200$ after 25 000 MCS, though we employ the data of $N=1599\times1600$ until 100 000 MCS.

NER of antiphase magnetization. Therefore, the system size is restricted to $N=1999\times2000$ at most. The NER function of fluctuation diverges algebraically at $T=T_c$, diverges exponentially at $T<T_c$ and remains finite at $T>T_c$. We find the phase transition temperature from these differences. It is noticed that the NER function finally converges to a finite value because the system is finite. Therefore, we must be aware of the range of time not to observe the finite-size effect. This is a time scale that the correlation length reaches the finite system size. We compare the NER functions of two different sizes ($1999\times2000$, $1599\times1600/1599\times1600$, $999\times1000/1599\times1600$, $799\times800$, etc.) for every data point, and estimate this crossover time until which two curves fall on the same line and the finite-size effect does not appear. An example of this comparison is shown in Fig. 6. The NER functions of the layer magnetization from the paramagnetic phase $m_l(t)$ are plotted for three sizes $N=1999\times2000$, $N=1599\times1600$, and $N=1199\times1200$ at $T=0.92$ and $\kappa=0.6$.

TABLE III. The crossover MCS at each temperature for $\kappa=0.6$ and 0.8. This is a MC step until which the NER function falls on the same line as that of a larger system.

| | $T$ | $L_x\times L_y$ | Crossover MCS |
|---|---|---|---|
| $\kappa=0.6$ | 0.88 | $999\times1000$ | $\sim$8000 |
| | 0.90 | $999\times1000$ | $\sim$10 000 |
| | 0.92 | $1599\times1600$ | $\sim$100 000 |
| | 0.95 | $999\times1000$ | $\sim$10 000 |
| | 0.97 | $799\times800$ | $\sim$8000 |
| | 1.00 | $999\times1000$ | $\sim$100 000 |
| $\kappa=0.8$ | 1.30 | $799\times800$ | $\sim$5000 |
| | 1.33 | $999\times1000$ | $\sim$10 000 |
| | 1.35 | $1199\times1200$ | $\sim$100 000 |
| | 1.40 | $599\times600$ | $\sim$8000 |
| | 1.50 | $599\times600$ | $\sim$100 000 |

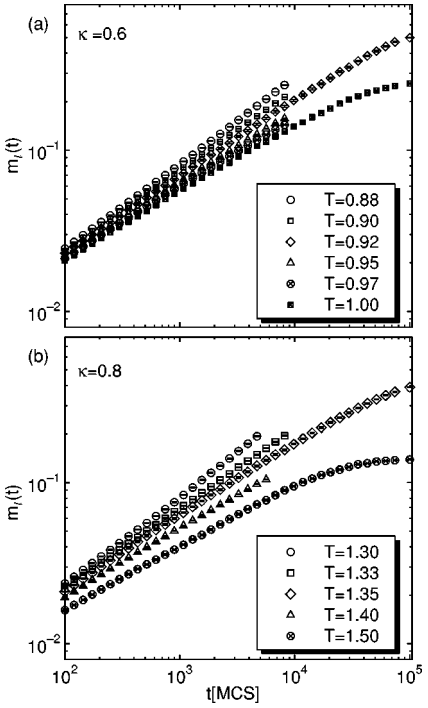


FIG. 7. The NER of layer magnetization $m_l(t)$, for (a) $\kappa=0.6$ and (b) $\kappa=0.8$ started from the paramagnetic state.

Three curves fall on the same line until 25 000 MCS. After this crossover time, however, the curve of $N=1199\times1200$ bends down from the other two curves, probably because the correlation length reaches 1200 at this temperature. So, we

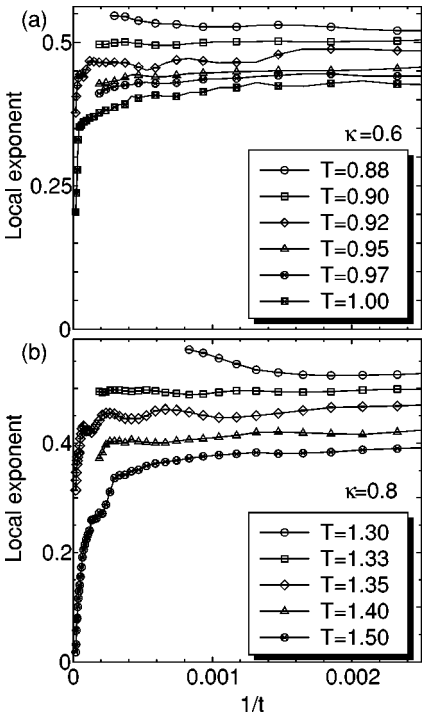


FIG. 8. The local exponent of the layer magnetization $m_l(t)$ for (a)$\kappa=0.6$ and (b)$\kappa=0.8$ started from the paramagnetic state. In both systems, local exponents converge to $\lambda=(2-\eta)/z=0.49$ in the limit of $t\to\infty$ at the transition temperature.

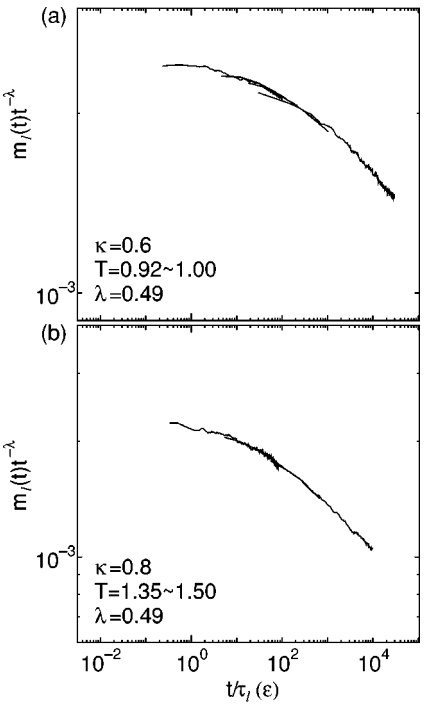


FIG. 9. The finite-time scaling of the layer magnetization $m_l(t)$ started from the paramagnetic state. The data of four different temperatures ranging $T=0.92-1.00$ are plotted together for (a) $\kappa=0.6$, while those of different three temperatures ranging $T=1.35-1.50$ are plotted for (b) $\kappa=0.8$

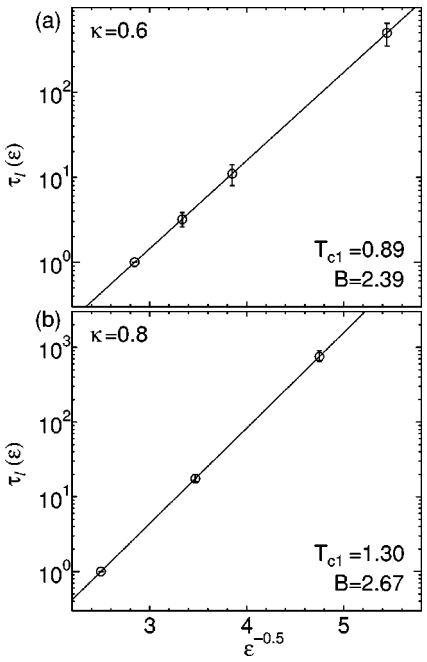


FIG. 10. The least-square fitting of the relaxation time $\tau_l(\varepsilon)$ by Eq. (11) for (a) $\kappa=0.6$ and (b) $\kappa=0.8$. The transition temperature is estimated to give the best fitting as (a) $T_{c1}=0.89$ and (b) $T_{c1}=1.30$.

have to discard the data of $N=1199\times1200$ after 25 000 MCS. Comparing two curves of $N=1999\times2000$ and $N=1599\times1600$, we can use the data of $N=1599\times1600$ until at least $10^5$ MCS. Table III shows the crossover MCS at each temperature for $\kappa=0.6$ and 0.8. Thus, we use a system of a proper size for a proper observing time at each temperature. We take averages over 1000–7000 independent MC runs.

The NER of the layer magnetization, $m_l(t)$, from the paramagnetic state are shown in Fig. 7 for (a) $\kappa=0.6$ and (b) $\kappa=0.8$. Figure 8 shows the corresponding local exponents. In Fig. 8(a), the exponent decreases for $T\geqslant0.92$ and diverges for $T\leqslant0.88$. At $T=0.90$, it converges to a finite value. In consequence, we predict that the phase transition temperature between the paramagnetic phase and the IC phase is $T_{c1}=0.90\pm0.02$. For $\kappa=0.8$, we obtained $T_{c1}=1.325\pm0.025$ as shown in Fig. 8(b).

Furthermore, we also analyze the upper transition temperature $T_{c1}$ using the finite-time scaling as shown in Figs. 9 and 10. We show the scaling in Fig. 9 for (a) $\kappa=0.6$ and (b) $\kappa=0.8$. Since the layer magnetization diverges algebraically as $t^{(2-\eta)/z}$ at the transition temperature, we plot $m_l(t)t^{-\lambda}$ against $t/\tau_l(\varepsilon)$. All the curves excellently fall on the same line, by which we obtain the relaxation time as shown in Fig. 10. Here, we adopt $\lambda=(2-\eta)/z=0.49$ that is a value which the local exponent converges to (see Fig. 8). If we admit the KT criterion $\eta=1/4$, the dynamic exponent is estimated as $z\sim3.6$. Next, we fit the relaxation time using Eq. (11). Figure 10 shows the best least-square fitting for (a) $\kappa=0.6$ and (b) $\kappa=0.8$. We obtain the transition temperature $T_{c1}=0.890\pm0.015$ for $\kappa=0.6$ and $T_{c1}=1.300\pm0.013$ for $\kappa=0.8$. These transition temperatures are again consistent with the values estimated from the local exponents of the NER from the paramagnetic state, and those by the scaling from the ground state.

Therefore, we are able to conclude that $T_{c1}$ and $T_{c2}$ coincide with each other within limits of error in both cases of $\kappa=0.6$ and 0.8. The phase transition temperature between the paramagnetic phase and the IC phase is $T_{c1}=0.895\pm0.025$ and that between the antiphase and the IC phase is $T_{c2}=0.89\pm0.02$ for $\kappa=0.6$, and $T_{c1}=1.32\pm0.03$ and $T_{c2}=1.32\pm0.02$ for $\kappa=0.8$. Since these temperatures are very close to each other, it is suggested that the IC phase does not exist or it is very narrow even if it exists. We need to pay attention to a fact that Monte Carlo simulation is not able to exclude a very tiny temperature region.

## IV. CONCLUSIONS

It has been considered that the successive phase transitions with a finite IC phase take place for $\kappa>0.5$ in two-dimensional ANNNI model. In this paper, we estimated the phase transition temperatures by applying the NER method, and found that the $T_{c1}$ is equal to $T_{c2}$ within limits of errors. This is a very exotic phase transition, which is the KT type if approached from the high-temperature side, and is the second-order if approached from the low-temperature side. Therefore, we speculate successive phase transitions with an *infinitesimal* IC phase may occur in this system.

In the studies of the C-IC transitions in two-dimensional systems, it has been investigated the systems with an asymmetric parameter which explicitly favors the IC

structure.[33–35] For a finite value of the parameter, there exists the finite IC phase between the commensurate phase and the paramagnetic phase. In the limit of vanishing the parameter, the IC phase shrinks to the infinitesimal. The frustration parameter $\kappa$ of the ANNNI model has been considered as the asymmetric parameter based on the approximate theory[12–17] valid only at low temperatures, and the small-scaled Monte Carlo simulations.[18–20] However, what is actually favored by frustration is the creation of the domain wall. Between the creation of the domain wall and the realization of the IC structure, there are many conditions to satisfy, which have been supposed in the free-fermion approximation.[13] One of these is the spin correlation along the ferromagnetic chain. In the two-dimensional ANNNI model, the nonfrustrated direction is only one dimension, and thus the spin correlation along the ferromagnetic chain can be easily destroyed. Therefore, we question regarding the frustration parameter as the asymmetric parameter. If we consider that these two are not related with each other and the asymmetric parameter is zero in the present model, the width of the IC phase becomes infinitesimal. This is what we observed in this paper.

Here, we show the comparison of the obtained transition temperatures with the previous ones in Table I. It is recognized that our $T_{c1}$ is lower than any other ones, though $T_{c2}$ is consistent with each other. This can be explained by the difference of the finite-size effect. The phase transition between the IC phase and the paramagnetic phase is confirmed to be the KT transition while the one between the antiphase and the IC phase is the second order. The correlation length diverges algebraically against the temperature in the latter, while it diverges exponentially in the former case. If a system size is small compared with the correlation length and the accuracy of the numerical data is not enough, even the finite-size scaling analysis may mislead to a wrong $T_c$, where the finite but very large correlation length reaches the finite system size. Therefore, it is very likely that the KT transition temperature obtained previously is overestimated. We may rather easily obtain the phase transition temperature accurately in the second-order transition, because the divergence is algebraically. In the two-dimensional ANNNI model, the correlation length along the chain direction is $\xi_x \sim 500$ at $T=1.40$ and $\kappa=0.8$ which is the temperature a little higher than the KT transition temperature and the correlation length is far larger than the system sizes ever simulated previously ($N=64\times128$).[20] We actually used data with system sizes $N=599\times600\sim6399\times6400$ in this paper, and checked the finite-size effect and the range of observing time in which the system behaves as an infinite system at each temperature. Thus, our data can be considered as closed to the thermodynamic value. This is a reason why we could detect the KT transition accurately.

In this paper, we have supposed that the ferromagnetic correlation along the chain direction remains finite or at least it is critical in the IC phase. Thus, the $T_{c1}$ we have obtained is the temperature at which the ferromagnetic correlation becomes critical. Above this temperature, each ferromagnetic chain exhibits paramagnetism, even though the correlation length is very large near the $T_{c1}$. The present results only exclude the finite IC phase of this type. In this study, it is clarified that the domain walls penetrate into the system along the chain direction at the lower transition temperature $T_{c2}$. The spin configuration along the chain direction changes drastically from the ferromagnetic ordered state to the paramagnetic disordered state at the same temperature within limits of error. We can neglect the IC phase where the ferromagnetic correlation has been expected to be critical. Therefore, the domain walls mostly run straight along the chain direction. We consider this is why the naive free-fermion approximation of Villain and Bak[13] gives the best quantitative agreements with our estimate of $T_{c2}$, and is the best approximation. The analyses for other regions of $\kappa$ and determination of the critical exponents will be a task in the future. The NER of the Binder parameter, the specific heat and the spin correlation with high accuracy is necessary.[22]

As for the dielectrics, $Pb(Zr_{1-x}Ti_x)O_3$, the phase diagram[3] in the low concentration of Ti is very similar to that of the ANNNI model if we interpret the paraelectric, the ferroelectric and the antiferroelectric phases as the paramagnetic, the ferromagnetic and the antiphase phases. There are two controversial explanations for the existence of the incommensurate phase observed in the experiment. Ricote *et al.*[4] concluded that the appearance of the IC phase is due to the surface effect by two experiments using the powder neutron diffraction and a transmission electron microscope. On the other hand, Viehland *et al.*[5] considered it a bulk effect by directly observing the high resolution image of a transmission electron microscope. In addition Watanabe *et al.*[6] also described that it is not because of the surface effect by examining the stability of the IC phase in the bulk. If this compound can be explained by the ANNNI model, the existence of the IC phase is only possible in three dimensions. Therefore, we predict that the appearance of the IC phase in $Pb(Zr_{1-x}Ti_x)O_3$ is the effect of a bulk.

In this work, we have presented that the NER analysis is very effective for systems with the KT transition and/or with slow dynamics which has been difficult by numerical methods. Furthermore, a phase transition is studied using the finite-time scaling if we know a proper quantity that can probe characteristic time, $\tau$, or a characteristic length $\xi$ even though it is not a relevant order parameter. It is considered that images of the phase transition which has been believed as standard may change in some systems.

## ACKNOWLEDGMENTS

The authors would like to thank Professor Fumitaka Matsubara, Professor Kazuo Sasaki, Professor Nobuyasu Ito, and Dr. Yukiyasu Ozeki for fruitful discussions and comments. They also thank Professor Nobuyasu Ito and Professor Yasumasa Kanada for providing us with a fast random number generator RNDTIK.

[1] S. Kawano and N. Achiwa, J. Magn. Magn. Mater. **52**, 464 (1985).
[2] R.J. Elliott, Phys. Rev. **124**, 346 (1961).
[3] X. Dai, Z. Xu, and D. Viehland, J. Am. Ceram. Soc. **78**, 2815 (1995).
[4] J. Ricote, D.L. Corker, R.W. Whatmore, S.A. Impey, A.M. Glazer, J. Dec, and K. Roleder, J. Phys.: Condens. Matter **10**, 1767 (1998).
[5] D. Viehland, Phys. Rev. B **52**, 778 (1995).
[6] S. Watanabe and Y. Koyama, Solid State Phys. (Tokyo) **35**, 880 (2000).
[7] V. Massidda and C.R. Mirasso, Phys. Rev. B **40**, 9327 (1989).
[8] J.M. Tranquada, B.J. Sternlieb, J.D. Axe, Y. Nakamura, and S. Uchida, Nature (London) **375**, 561 (1995).
[9] P. Bak and J. von Boehm, Phys. Rev. B **21**, 5297 (1980).
[10] M. Matsuda, K. Katsumata, T. Yokoo, S.M. Shapiro, and G. Shirane, Phys. Rev. B **54**, R15 626 (1996).
[11] H.F. Fong, B. Keimer, J.W. Lynn, A. Hayashi, and R.J. Cava, Phys. Rev. B **59**, 6873 (1999).
[12] E. Müller-Hartmann and J. Zittartz, Z. Phys. B: Condens. Matter **27**, 261 (1977).
[13] J. Villain and P. Bak, J. Phys. (Paris) **42**, 657 (1981).
[14] J. Kroemer and W. Pesch, J. Phys. A **15**, L25 (1982).
[15] M. D. Grynberg and H. Ceva, Phys. Rev. B **36**, 7091 (1987).
[16] M.A.S. Saqi and D.S. McKenzie, J. Phys. A **20**, 471 (1987).
[17] Y. Murai, K. Tanaka, and T. Morita, Physica A **217**, 214 (1995).
[18] W. Selke and M. E. Fisher, Z. Phys. B: Condens. Matter **40**, 71 (1980).
[19] W. Selke, Z. Phys. B: Condens. Matter **43**, 335 (1981).
[20] A. Sato and F. Matsubara, Phys. Rev. B **60**, 10 316 (1999).
[21] N. Ito, Physica A **192**, 604 (1993).
[22] N. Ito and Y. Ozeki, Int. J. Mod. Phys. C **10**, 1495 (1999).
[23] N. Ito, K. Hukushima, K. Ogawa, and Y. Ozeki, J. Phys. Soc. Jpn. **69**, 1931 (2000).
[24] N. Ito, T. Matsuhisa, and H. Kitatani, J. Phys. Soc. Jpn. **67**, 1188 (1998).
[25] Y. Ozeki and N. Ito, J. Phys. A **31**, 5451 (1998).
[26] N. Ito, Y. Ozeki, and H. Kitatani, J. Phys. Soc. Jpn. **68**, 803 (1999).
[27] K. Ogawa and Y. Ozeki, J. Phys. Soc. Jpn. **69**, 2808 (2000).
[28] Y. Nonomura, J. Phys. Soc. Jpn. **67**, 5 (1998).
[29] Y. Nonomura, J. Phys. A **31**, 7939 (1998).
[30] Y. Ozeki, N. Ito, and K. Ogawa (unpublished).
[31] Y. Ozeki, K. Ogawa, and N. Ito (unpublished).
[32] J.M. Kosterlitz and D.J. Thouless, J. Phys. C **6**, 1181 (1973).
[33] H.J. Schulz, Phys. Rev. B **28**, 2746 (1983).
[34] W. Selke and J.M. Yeomans, Z. Phys. B: Condens. Matter **46**, 311 (1982).
[35] S. Ostlund, Phys. Rev. B **24**, 398 (1981).
[36] M. Suzuki, Prog. Theor. Phys. **58**, 1142 (1977).
[37] A. Jaster, J. Mainville, L. Schülke, and B. Zheng, J. Phys. A **32**, 1395 (1999).
[38] A. Sadiq and K. Binder, J. Stat. Phys. **35**, 517 (1984).